Sap flow and water use sources of shelter-belt trees in an arid inland river basin of Northwest China

Second version of revised manuscript submitted to *Ecohydrology* (ECO-14-0070)

Qin Shen [1, 2], Guangyao Gao [1, *], Bojie Fu [1], YiheLü [1]

[1] *State Key Laboratory of Urban and Regional Ecology, Research Center for Eco-Environmental Sciences, Chinese Academy of Sciences, Beijing 100085, China*

[2] *University of Chinese Academy of Sciences, Beijing 100049, China*

*Corresponding to: Guangyao Gao

State Key Laboratory of Urban and Regional Ecology, Research Center for Eco-Environmental Sciences, Chinese Academy of Sciences, Beijing 100085, China.

E-mail: gygao@rcees.ac.cn

This article has been accepted for publication and undergone full peer review but has not been through the copyediting, typesetting, pagination and proofreading process, which may lead to differences between this version and the Version of Record. Please cite this article as doi: 10.1002/eco.1593

ABSTRACT

The knowledge of plant water use characteristics was essential for ecosystem management and water resources distribution in arid inland river basin. This study was conducted to quantify the sap flow variations and water use sources of shelter-belt trees at the oasis-desert ecotone in the middle of China's Heihe River Basin. Sap flow was measured by the thermal dissipation method on eight Gansu Poplar (*Populus gansuensis*) trees with different diameter at breast height (DBH) in 2012 and 2013. The mean sap flow density increased linearly with DBH. The sap flow density exhibited linear relationship with solar radiation, and it increased logarithmically with vapor pressure deficit and air temperature, whereas the water table had negative impact on sap flow. The relationship between sap flow and soil relative extractable water at 0-220 cm depth was implicit during the whole growing season, whereas the soil water had apparently positive influence on sap flow after the shelter-belt trees irrigation. The stand transpiration rate represented as a logarithmic function of reference crop evapotranspiration. The total transpiration of Gansu Poplar during growing season was 599.3 mm, whereas only 58.1% of which was provided by the precipitation and irrigation. The groundwater and cropland irrigation were critical water sources of shelter-belt trees. The contribution of groundwater to tree transpiration was estimated to be 35.1% and 19.0% in 2012 and 2013, respectively. The great precipitation in 2013 weakened the dependence of tree transpiration on groundwater. The estimated threshold distance of cropland irrigation influencing the

tree transpiration was about 8 m.

KEY WORDS shelter-belt trees; sap flow; transpiration; soil water; groundwater; Heihe River Basin

INTRODUCTION

Water scarcity is serious in arid and semiarid areas due to limited supplies and increasing demand because of great population growth (Scanlon *et al*., 2005). Water availability is considered to be a restricting factor for plant growth. Evaluating plant water use characteristics and understanding plant responses to water deficits are essential for water resources and ecosystem sustainable management. Plant transpiration is the key to understand the dynamic water use characteristics.

Plant transpiration was studied in various arid and semiarid areas over the world with different precipitation and groundwater conditions (Table I). These studies focused on the characteristics of plant transpiration and the relationships between environmental factors and plant transpiration. However, the identification and quantification of various water use sources for plant transpiration need further investigation. This study is attempting to fill this knowledge gap.

The investigation of influencing factors on plant transpiration is important to comprehensively understand the water use characteristic. There are many factors influencing tree sap flow, including meteorological factors, soil water and groundwater. The main meteorological factors were solar radiation and vapor pressure deficit (Sellami *et al*., 2003). The sap flow was shown to have a positive relationship with solar radiation (Chen *et al*., 2014), whereas the response of sap flow to vapor pressure deficit showed a complex behavior. The sap flow increased linearly with vapor pressure deficit (Gazal *et al*., 2006), or increased within a threshold and subsequently reached an

asymptotic value (Du *et al*., 2011) or declined (Chirino *et al*., 2011). Some other meteorological factors such as air temperature (Rousseaux *et al*., 2009), rainfall pulses (Zhao and Liu, 2010) and wind speed (Chu *et al*., 2009) could also influence sap flow.

In addition, soil water was thought to be a critical factor affecting tree sap flow in arid and semiarid areas where plants were always in water deficit conditions (Zhao and Liu, 2010; Naithani *et al*., 2012). Soil water conditions could restrict many tree physiological processes, whereas temporal recharge of soil water by rainfall or irrigation caused sap flow acceleration due to a release of xylem hydraulic conductance (Eberbach and Burrows, 2006; Du *et al*., 2011). Sap flow of desert shrubs (*Nitraria sphaerocarpa* and *Elaeagnus angustifolia*) represented a polynomial relationship with soil water at the depth of 0-20 cm (Zhao and Liu, 2010). Some studies also showed that sap flow increased linearly with soil moisture below a threshold, and no evident relationship was observed above the threshold (Zhang *et al*., 2011). However, some researches did not find constraints of soil water on sap flow, especially for plants with deep root, which was attributed to the root distribution and the ability of trees to access to groundwater (Prieto *et al*., 2010).

Groundwater was a critical factor influencing tree sap flow in shallow water table area. Current research about groundwater uptake by plant in arid area concentrated on riparian forests which could access to the shallow aquifers (Scott *et al.*, 2000; Gazal *et al*., 2006). Some studies showed that sap flow increased with decreasing water table depth (Gazal *et al*., 2006; Ma *et al*., 2013). However, a study of shelter-belt trees

planted with *Eucalyptus kochii* at three positions with shallow, deep and non-access to groundwater showed that sap flow appeared to be irrelevant to groundwater availability, whereas transpiration efficiency in terms of biomass accumulation decreased with declining groundwater availability (Brooksbank *et al*., 2011).

In the inland river basin of arid region, the shelter-belt trees are indispensable to the sustainability of the oasis-desert ecosystems, and play an important role in maintaining the security and stability of the oasis (Luo *et al*., 2005). The Heihe River is one of the largest inland rivers in the arid zones of Northwest China. In the middle reaches of Heihe River Basin, the Gansu Poplar, characterized by rapid growth, wind-sheltering and drought resistance, was planted as cropland shelter-belt trees (Chang *et al*., 2006). The sap flow and tree conductance of Gansu Poplar were conducted by Chang *et al*. (2006). Their study focused on the effects of meteorological factors on transpiration rate and tree conductance. More importantly, the amount of precipitation plus irrigation and soil water was insufficient to supply the transpiration (Chang *et al*., 2006). This result suggested the contribution from groundwater and nearby cropland lateral seepage for water consumption of shelter-belt trees. How much contribution of the groundwater could attribute to Gansu Poplar transpiration? How could the cropland irrigation affect the Gansu Poplar transpiration? In view of these concerns, we hypothesized that groundwater and soil water controlled the variations of the shelter-belt trees transpiration in addition to meteorological factors, and cropland irrigation could influence the Gansu Poplar within certain distance. The

focus of this study was to investigate the integrated effects of soil water, groundwater and cropland irrigation on sap flow of shelter-belt trees, which was not paid enough attention in previous studies.

To test these hypotheses, daily sap flow was measured by the thermal dissipation method on eight Gansu Poplar trees with different diameter at breast height in Heihe River Basin during two growing seasons in 2012 and 2013. The objectives of this study were to (1) investigate the influences of meteorological factors, soil water and water table depth on sap flow of Gansu Poplar shelter-belt trees, (2) determine the contributions of soil water and groundwater to transpiration of Gansu Poplar and (3) identify the roles of different water use sources of Gansu Poplar.

MATERIALS AND METHODS

Site description

The study area is located in a desert-oasis ecotone in the middle reach of Heihe River Basin, in Linze County of Gansu province, China (39°21′ N, 100°07′ E, altitude 1374 m). The area has a continental arid temperate climate with an average annual rainfall of 116.8 mm. The potential evaporation is 2390 mm $year^{-1}$, and the dryness index (potential evaporation divided by precipitation) is 20.46. The average annual temperature is 7.6 ^{o}C, and the highest and lowest temperatures are about 39.1 ^{o}C in July and -27.3^{o}C in January, respectively. The growing season is from May to October, and the frost-free period is about 165 days. The wind direction is mainly from the northwest, and the average wind speed is 3.2 m s^{-1} with frequent gales. The main soil

types are greyish-brown desert soil, sandy loam and sandy soil (Liu *et al*., 2009). The site geology is characterized by the multilayer structure constituted by gigantic rock debris and water-bearing rocks. The groundwater layer can be divided into upper and lower parts. The upper part is the shallow unconfined aquifer. The lower part is the multi-layered structure. More details about the site geology and aquifer conditions were described in Liu *et al*. (2009). The main vegetation types at the desert-oasis ecotone are composed of poplar shelter-belt trees, shrub sand-fixation forest and some desert vegetation, including *Populus Gansuensis, Populus bolleana*, *Calligonum mongolicum, Hedysarum scoparium, Tamarix chinensis, Nitraria sphaerocarpa*, *Reaumuria soongorica, Bassia dasyphylla*, *Halogeton arachnoideus, Suaeda glauca, Agriophyllum squarrosum, and Eragrostis pilosa* (Su *et al*., 2010).

The experiment was conducted in a shelter-belt trees stand of Gansu Poplar planted in 1982 during two consecutive growing seasons in 2012 and 2013. The topography was flat. The understory vegetation was sparse, and some *Phragmites communis*, *Tribulus terrestris*, *Sonchus oleraceus*, *Astragalus adsurgens*, *chenopodium album* were found. The shelter-belt trees were bounded on the north by desert and on the south by cropland. The shelter-belt trees were irrigated under conventional flood irrigation on June 20 in 2012 and May 19 in 2013 with the irrigation amount of about 250 mm. The cropland was irrigated every 7 to 14 days with the irrigation amount of approximate 100 mm each time. There were ten irrigation events in cropland in each year. The more details about the experimental site

can be found in Shen *et al*. (2014).

Sap flux and transpiration measurements

A plot (20 m length×12 m width) with 34 individual trees was chosen. Eight trees were selected with different diameters at breast height (DBH, cm), ranging from 21 to 38 cm. The selected eight trees covered the full range of tree diameter classes in the plot. The overview of the eight sample trees was shown in Table II. The changes in the tree DBH over the two years were slight and could be ignored. The sap flux was measured using the thermal dissipation method with constant heat flow gauges. Sap flow density was monitored with Granier type thermal dissipation sensors (TDP30, Rain Root Scientific Limited Company, Beijing, China) on the eight sample trees during the growing season in 2012 and 2013.

Each TDP sensor consisted of a pair of 30 mm-long and 1.2 mm-diameter probes. Each probe contained a copper-constantan thermocouple. Two sensors were inserted radially into the stem at breast height on the north and south side of the stem, respectively, to eliminate the error of the natural temperature gradient. The sensor on the north side of stem was used to measure the temperature difference between the two probes. The upper probe with a heater was supplied with a constant power of 2.5 V and the lower probe was used for an unheated reference. The other sensor on the south side of the stem with two unheated probes was used to measure the natural temperature. An aluminum foil covered the probes and tree trunk to avoid solar radiation and reduce effects of ambient temperature fluctuations.

Sap flow density (SF_d) on sapwood area basis was calculated based on the temperature difference between the heated and unheated probes by an empirical calibration equation determined by Granier (1985):

$$SF_d = 428.36[(\Delta T_{\max} - \Delta T)/\Delta T]^{1.231} \quad (1)$$

where SF_d was sap flow density (kg m^{-2} h^{-1}), ΔT was the temperature difference between the heated and unheated probes (^oC), and $\Delta T_{\max}$ was the maximal temperature difference with zero sap flow assumed at night (^oC). This assumption of zero sap flow seemed reasonable as that nighttime vapor pressure deficits were mostly low and temperature courses of sensors reached equilibrium at most nights (Dierick and Hölscher, 2009). Temperature differences were monitored at 10-s intervals and logged every 10-min averages. Granier (1985) indicated that the response of the TDP sensor was independent of the tree species. It was believed that the commonly used calibration function of Eq. (1) was valid for the Gansu Poplar in this study.

Sap flux (SF) was derived from the product of the sap flow density by the sapwood area (A_s, cm^2), based on the assumption of a uniform radial sap flow profile. The A_s was estimated from a regression relationship with the DBH (A_s=25.91DBH-311.96, R^2=0.94). The A_s and DBH were measured from the nearby cut trunks with circumferences ranging from 15 to 35 cm. The distinction between sapwood and heartwood was identified by the difference in color. The calculated total sapwood area in the plot was 1.56 m^2.

With the obtained average daily SF of the eight sample trees, the relationship

between *SF* and DBH was determined, which could be well described by a linear equation as indicated in the Results section. This relationship was applied to calculate sap flux for all other individual trees in the plot. Summing all tree sap flux and dividing this sum by the crown projected area of the plot could determine the stand transpiration during the growing season.

Meteorological variables

Relative humidity, air temperature, solar radiation, wind speed, atmospheric pressure and precipitation were measured by an AG1000 automatic weather station (Onset Computer Corporation, Pocasset, MA, USA) with about 300 m distance from the site. The meteorological data were recorded every 5 min with a CR1000 data logger (Campbell Scientific Inc., Logan, UT), and then stored as the 30-min mean data, whereas precipitation and wind data were stored every 10-min. Throughfall of the shelter-belt trees was collected by four rainfall tipping buckets with 16.5 cm-diameter and 24 cm-height (HOBO, Onset Computer Corporation, USA). Two rainfall tipping buckets were installed under the dense canopy and the other two ones were under the sparse canopy. The vapor pressure deficit (VPD, KPa) was calculated with the following equations:

$$\mathrm{VPD} = e_s(1 - RH) \tag{2}$$

$$e_s = 0.611\exp(\frac{17.27T_a}{237.3+T_a}) \tag{3}$$

where e_s was saturation vapor pressure (KPa), RH was relative humidity, and T_a was air temperature (^{o}C).

Daily reference evapotranspiration (ET_0, mm) was estimated using the FAO 56 Penman-Monteith equation (Allen *et al*., 1998):

$$ET_0 = \frac{0.408\Delta(R_n - G) + \gamma \frac{900}{T_a + 273} u_2 (e_s - e_a)}{\Delta + \gamma(1 + 0.34u_2)} \quad (4)$$

where R_n was net radiation at the crop surface (MJ m^{-2} day^{-1}), G was soil heat flux density (MJ m^{-2} day^{-1}), T_a was mean air temperature at 2 m height (^oC), u_2 was wind speed at 2 m height (ms^{-1}), e_s was saturation vapor pressure (KPa), e_a was actual vapor pressure (KPa), Δ was slope vapor pressure curve (KPa $^oC^{-1}$) and γ was the psychrometric constant (KPa $^oC^{-1}$).

Soil moisture and groundwater table

Soil moisture was monitored with six Trime-TDR access tubes (4-cm diameter, polycarbonate) with 4 m distance interval in the shelter-belt trees stand. The soil moisture profile was measured at 20 cm intervals to the depth of 2.8 m periodically (every 5 days) based on TDR (TRIME-TDR-PICO-IPH-T3, Imko, Germany). Additional measurements were made after the rainfall or irrigation events. It should be noted that soil moisture data used in the following analysis was the average value of the six tubes, which could represent the soil water condition of the plot. Soil moisture was calibrated by the oven drying method. Soil water storage (S, mm) was calculated by:

$$S = \sum_{i=1}^{n} (\theta_i . Z_i) \quad (5)$$

where θ_i was the volumetric soil moisture of ith layer (cm^3 cm^{-3}), Z_i was the thickness

of *i*th soil layer (cm), and *n* was the number of soil layers considered.

Soil relative extractable water (REW) was calculated based on the following equation (Granier, 1987):

$$\mathrm{REW} = \frac{\theta - \theta_{wp}}{\theta_{fc} - \theta_{wp}} \quad (6)$$

where θ_{wp} and θ_{fc} was the wilting coefficient and field capacity, which were equal to soil moisture at -1500KPa and -33 KPa in the soil water characteristic curve, respectively. During the study period, REW=0.4 was considered to be the threshold of soil moisture deficit (Granier, 1987; Chirino *et al*., 2011).

One groundwater table monitoring well was established in the shelter-belt trees stand. The depth to groundwater was automatically recorded every 20 min by water lever logger (Hobo U20-001-04, Onset Computer Corporation, Bourne, USA).

Soil properties and root distribution

A trench (320 cm deep × 400 cm length × 80 cm width) was dug in the shelter-belt trees stand. The undisturbed soil samples were taken from the soil profile every 20 cm depth with three replications using standard pre-weighed 100 ml Kopecki rings (a core sampling device). Soil samples were collected to analyze soil water characteristic curve (Hitachi-CR21G, Hitachi, Japan), soil mechanical composition (Mastersizer 2000, Malvern Instruments, England) and soil bulk density (oven drying method). The obtained soil physical properties of different soil layers in the shelter-belt trees stand were shown in Table III.

Soil columns with 20 cm depth were taken from the whole profile to pick tree

roots. The roots were observed up to 320 cm depth with approximately 90% of the fine root biomass (<2 mm) at the depth of 0-140 cm, and 41% of fine root concentrated in surface soil layer (0-20 cm) (Figure 1). Lateral roots of Gansu Poplar in the cropland were found with a distance of about 18 m from the cropland by trenches dug in the cropland.

Estimation of groundwater and soil water contributions to stand transpiration

The amount of groundwater and soil water uptake for trees transpiration was calculated by the soil mass balance approach according to Pinto *et al*. (2013) based on that trees used soil water preferentially and subsequently groundwater when the soil water storage was not enough for transpiration. Three additional assumptions were made. First, surface runoff was neglected because of the flat topography of the experimental plot and the high infiltration capacity of soil. Second, the understory evapotranspiration was not considered since the soil moisture was always in a deficit condition and the understory species was sparsely diffused. Furthermore, the lateral soil water movements between shelter-belt trees and cropland were not accounted for due to non-available data to quantify it. Calculations were run in daily with the following procedures.

Firstly, the changed soil water storage (S_1) was calculated by:

$$S_1 = S_0 + TF - T \quad (7)$$

where S_0 was the initial daily soil water storage (mm), *TF* was the throughfall (mm),

and T was the stand transpiration (mm).

Secondly, groundwater recharge (G_r, mm), groundwater uptake (G_{up}, mm) and soil water uptake (S_{up}, mm) was calculated as follows:

$$G_r = \begin{cases} S_1 - S_{fc} & S_1 > S_{fc} \\ 0 & S_1 \le S_{fc} \end{cases} \quad (8)$$

$$G_{up} = \begin{cases} S_{wp} - S_1 & S_1 < S_{wp} \\ 0 & S_1 \ge S_{wp} \end{cases} \quad (9)$$

$$S_{up} = T - G_{up} \quad (10)$$

where S_{fc} (mm)and S_{wp} (mm) was the soil water storage at field capacity and wilting point, respectively.

Finally, the contribution of groundwater (r_g) and soil water (r_s) to tree transpiration were calculated by:

$$r_g = \frac{\sum_{j=1}^{m} G_{up\_j}}{\sum_{j=1}^{m} T_j} \quad (11)$$

$$r_s = \frac{\sum_{j=1}^{m} S_{up\_j}}{\sum_{j=1}^{m} T_j} \quad (12)$$

where G_{up_j} was the groundwater uptake of jth day (mm), S_{up_j} was the soil water uptake of jth day (mm), T_j was the transpiration of jth day (mm), and m was the number of days during the study periods.

Statistical analyses

The effects of air temperature, solar radiation, vapor pressure deficit, relative

humidity, precipitation and water table depth on sap flow density were investigated by correlation analysis and stepwise regression analysis. SPSS® (version 18.0) was used for all statistical analyses.

RESULTS

Climate, water table depth and soil moisture

There was little difference in daily mean air temperature during the growing season (May-October) between 2012 (20.8 ^{o}C) and in 2013 (20.2 ^{o}C). Air temperature of June, July and August were higher than other two months. Daily mean vapor pressure deficit and solar radiation was 1.5 KPa and 22.7 MJ m^{-2} in 2012, reducing to 1.4 KPa and 20.5 MJ m^{-2} in 2013. Daily mean relative humidity was 40% in 2012 and 43% in 2013. During the growing season, there were 22 and 24 rainfall events in 2012 and 2013, which produced a total rainfall of 90.6 mm and 105.6 mm, respectively (Figure 2). The heaviest rainfall occurred on June 5 of 2012 (16.2 mm) and July 14 of 2013 (30.6 mm).

Water table depth fluctuated with the irrigation events and water level of Heihe River. At the commencement of the study period in 2012, water table depth fell and reached the lowest value of 3.6 m on June 3. Then it began to rise and reached the peak with the value of 2.9 m on June 28 after large amount irrigation in the shelter-belt trees. Afterwards, water table depth declined to 3.9 m at the end of the first study period. During the next study period of 2013, water table depth declined to the lowest value of 3.6 on May 18, and rose to the highest value of 2.9 m on May 20,

then it fluctuated around 3.3 m and declined to 3.6 m at the end of the study period (Figure 2). The rose of water table depth always lagged about one or two days behind the irrigation occurrence.

The vertical distribution of mean soil moisture during growing seasons in 2012 and 2013 was given in Figure 1. The soil moisture profile composed of two distinct layers. At 0-220 cm depth, there was slight difference between soil moisture at different layers with the value of around 7.16%. At the lower layer below 220 cm depth, the soil moisture significantly increased with depth, ranging from 10.09% to 27.92%. Soil moisture temporal variations of different layers (0-20 cm, 20-160 cm, 160-220 cm and 220-280 cm) in 2012 and 2013 were shown in Figure 3a. At the upper three soil layers, soil moisture increased with some pulses due to the shelter-belt trees irrigation and large rainfall events. In the lowest layer (220-280 cm), soil moisture varied with the water table depth, with the value (>25.34%) higher than field capacity (20.38%). Therefore, soil water storage of unsaturated soil layer at 0-220 cm depth was used to calculate soil water uptake by trees with the soil mass balance approach aforementioned. The temporal variations of REW and soil water storage at the depth of 0-220 cm were shown in Figure 3b. REW varied similarly as the soil moisture, with the value lower than 0.4 during most of the study period in 2012, whereas in 2013 the soil water deficit condition of the upper unsaturated zone mainly occurred in the late period of the growing season.

Diurnal variation of sap flow

The diurnal variation in sap flow density followed a unimodal curve (Figure 4). The sap flow density was lower at night, increased sharply between 6:00 and 8:00 h, and reached a maximum value between 13:00 and 14:00 h. As shown in Figure 4, the diurnal course of sap flow density was closely related to the changes of solar radiation and vapor pressure deficit. The peak of sap flow density occurred at nearly same time as the maximum solar radiation but somewhat earlier than maximum vapor pressure deficit (Figure 4). The daily pattern of sap flow density was similar among trees with different diameter at breast height and different distance from the cropland, as evident from Figure 4b.

The sap flow density of individual sample trees showed significant differences ($p < 0.01$), with the value ranging from 30.62±11.44 to 101.88±28.98 kg m^{-2} h^{-1}. Furthermore, the relationship between average daily sap flow density (SF_d) and tree diameter at breast height (DBH) could be well described by a linear equation (SF_d=3.72DBH -35.67, R^2=0.64). The mean daily sap flux (SF) varied more than tenfold among the individual Gansu Poplar trees, with the value of 17.06 kg day^{-1} by smallest tree with respect to 164.50 kg day^{-1} consumed by the largest tree. Similar to SF_d, the SF increased linearly with the DBH (SF=8.38DBH-158.48, R^2=0.92). This relationship was used to upscale the tree transpiration to plot scale and determine the stand transpiration.

Relationship between sap flow and environmental factors

During the growing season, sap flow density was positively correlated with air temperature, solar radiation, vapor pressure deficit and REW, whereas it was negatively correlated with water table depth in both 2012 and 2013 (Table IV). The sap flow density represented linear relationship with solar radiation and water table depth (Figures 5a and 5d), where it represented logarithmic relationship with air temperature and vapor pressure deficit (Figures 5b and 5c).

The relationship between sap flow density and REW was not clear during the whole growing season (Figure 5e). In dry soil water condition, the sap flow density fluctuated significantly between minimum and maximum values, whereas it always retained at large value in wet soil water condition. Gansu Poplar reached its maximum sap flow density in summer, even though REW was at a minimum during this period because of the seasonal variation. However, the effect of soil water on sap flow density was apparent by the shelter-belt trees irrigation. The sap flow density was significantly different between pre-irrigation and post-irrigation with the mean value of 84.90 and 92.87 kg m^{-2} h^{-1}, respectively ($p < 0.05$). The regression linear line between daily sap flow density and solar radiation during post-irrigation lied above that during pre-irrigation (Figure 6a). The sap flow density represented a polynomial relationship with vapor pressure deficit (Figure 6b), which was different from the logarithmic relationship during the whole growing season. The sap flow density during post-irrigation increased significantly with respect to that during pre-irrigation

under similar meteorological conditions, which was due to the sharp increase of soil moisture after shelter-belt trees irrigation as shown in Figure 3.

Correlation between stand transpiration and reference crop evapotranspiration

The daily stand transpiration rate represented a significantly logarithmic relationship with reference crop evapotranspiration, with a correlation coefficient of 0.72 in 2012 and 0.54 in 2013 (Figure 7). The stand transpiration rate increased with reference crop evapotranspiration, then reached a plateau at high reference crop evapotranspiration, which was similar to the relationship between sap flow density and vapor pressure deficit. This result was ascribed to that the high vapor pressure deficit could restrict canopy conductance by stomatal closure, and hence impede the stand transpiration (Chang *et al*., 2006).

Contributions of groundwater and soil water to stand transpiration

During the growing season, total stand transpiration was 604.5 mm in 2012 and 594.1 mm in 2013, with the average value of 4.9 mm d^{-1} in 2012 and 4.8 mm d^{-1} in 2013, respectively. The average stand transpiration was somewhat higher than the result obtained by Chang *et al.* (2006) with the value of 4.1 mm d^{-1}. This was due to that the DBH of studies trees (21~38 cm) was higher than that (18~31 cm) in Chang *et al*. (2006). Therefore, it could be believed the obtained stand transpiration in this study was reasonable. The groundwater and soil water uptake accounted for 35.14%

and 64.86% of tree transpiration in 2012, respectively. The corresponding contribution of groundwater and soil water in 2013 was 18.99% and 80.01%, respectively. Soil water took up a large proportion of transpiration because of the shelter-belt trees flood irrigation during these periods. Furthermore, the more precipitation in 2013 resulted in the reduction of sap flow dependence on groundwater with respect to 2012.

DISCUSSION

Effects of environmental factors on sap flow

The variations of sap flow are controlled by stomatal conductance. The stomatal conductance is regulated not only by physiological characteristics of plants such as canopy structure, sapwood area and hydraulic architecture (Pataki *et al*., 2000; Tognetti *et al*., 2004), but also by environmental factors such as solar radiation, vapor pressure deficit, soil water and groundwater (Cooper *et al*., 2003; Motzer *et al*., 2005; Liu *et al*., 2011).

The results revealed that solar radiation and vapor pressure deficit jointly affected sap flow. The diurnal variation of sap flow density showed similar patterns with solar radiation and vapor pressure deficit (Figure 4). The daily mean sap flow density increased with increasing solar radiation or vapor pressure deficit, while sap flow density reached a plateau at high vapor pressure deficit (Figures 5a and 5c). Similar results were found in a lower tropical montane rain forest at vapor pressure deficit larger than 1.0-1.2 KPa (Motzer *et al*., 2005), and a subalpine forest stand in the central Rocky Mountains at vapor pressure deficit larger than 1.8 KPa (Pataki *et al*.,

2000). They attributed the limiting effect of high vapor pressure deficit on transpiration to the closure of stomata. Chang *et al*. (2006) proved that tree conductance of Gansu Poplar decreased exponentially with increasing vapor pressure deficit.

The regulation of stomatal conductance was also dependent on soil water condition besides the vapor pressure deficit (Chen *et al*., 2013). It was reported that the influence of soil water on stomatal regulation might surpass that of vapor pressure deficit when soil was in a continuous dry condition (Tognetti *et al*., 2004). The sap flow density in *Abies lasiocarpa* decreased by 50% in late season, which was due to the closed stomata caused by soil water deficit (Pataki *et al*., 2000). However, in contrary to previous studies, the relationship between sap flow density and soil relative extractable water was implicit as shown in Figure 5e. This was due to that the seasonal variation weakened the effect of soil water on stomatal conductance during the whole growing season. The little evidence for soil water control over sap flow density was against the proposed hypothesis in this study that soil water condition was a key factor controlling tree transpiration. Therefore, the variations of sap flow density during the whole growing season were mainly controlled by meteorological factors in addition to water table depth. However, the shelter-belt trees irrigation resulted in the sharp increase of soil moisture, which could significantly increase the sap flow density (Figure 6). The explicit relationship between tree conductance and soil water need further investigation.

The presence of deep shelter-belt trees root system buffered the effect of reductions in REW, and thus maintained sufficient water supply for tree transpiration, which resulted in the increase of sap flow density with decreasing water table depth (Figure 5d). Similar result was found in the middle and lower reaches of the Tarim River in *Populus euphratica* (Ma *et al*., 2013). The access to groundwater determined tree physiological response to water table depth (Chen *et al*., 2013). However, this phenomena occurred only at appropriate water table depth. This was supported by the finding of Gazal *et al*. (2006) who compared tree transpiration at two sites (intermittent and perennial stream site). Lower rates of transpiration corresponded with greater depths to groundwater were found at the intermittent stream site, whereas it was not observed at the perennial stream site.

Water sources for tree transpiration

In this study, the amount of precipitation and irrigation (340.6 mm in 2012 vs. 355.6 mm in 2013) was inadequate to supply the transpiration of Gansu Poplar (604.5 mm in 2012 vs. 594.1 mm in 2013) during the growing season. The shelter-belt trees needed to use water from other sources. As shown in Figures 1 and 2, the roots of Gansu Poplar could access to the groundwater. During the growing season, the groundwater uptake accounted for 35.14% and 18.99% of tree transpiration in 2012 and 2013, respectively. Pinto *et al*. (2013) estimated the yearly groundwater contribution to tree transpiration of *Quercus suber* to be 30.3%, while groundwater uptake became dominant in the dry summer to account for 73.2% of tree transpiration.

The relative contribution of groundwater and soil water to tree transpiration was affected by the rainfall condition. The more precipitation in 2013 recharged the soil water and weakened the dependence of tree transpiration on groundwater in this study. Cramer *et al*. (1999) found that groundwater was the dominant water source of *Casuarina glauca* transpiration during the whole study period (over 70%), while groundwater occupied only 40% of transpiration during period with high rainfall. Vincke and Thiry (2008) found that the contribution of groundwater to Scots pine stand (*Pinus sylvestris*) transpiration during May-November was 61%, while the contribution reached 98.5% during the drought period in June. Gou and Miller (2013) indicated that the dominant water source for blue oaks (*Quercus douglasii*) transpiration in California savanna turned from groundwater in the dry season to soil water in the wet season.

The cropland irrigation was another water source for trees in addition to soil water and groundwater in the shelter-belt. The sap flux of trees adjacent to the cropland was ten times larger than that of trees away from the cropland. The trees in edge of the shelter-belt trees stand could absorb soil water diffused from cropland, or extended the roots into the cropland. The transpiration variations of six trees at different distances from the cropland (6.0, 6.3, 7.6, 8.1, 13.5 and 14.8 m) for three days after the cropland irrigation event were shown in Figure 8. It could be found that after irrigation events in the cropland, the sap flow density of Gansu Poplar with distance of 6.0 m, 6.3 and 7.6 m from the cropland had a sharp increase. The increase of sap

flow density was slight for the tree with distance of 8.1 m away from the cropland, whereas there were no increase and even a drop for the trees with 13.5 m and 14.8 m distance from cropland. The responses in transpiration on more than a single one day for several trees could explicitly support that the trees could use cropland irrigation soil water. It appeared that the cropland irrigation could influence the transpiration of the shelter-belt trees within a distance of about 8 m from the cropland.

Limitation and implications of this study

This study supported the proposed hypothesis that the groundwater was an important water use source of Gansu Poplar. Furthermore, the response of tree transpiration was subjected to the adjacent cropland irrigation within a threshold distance of about 8 m. The contribution of different water sources for Gansu Poplar transpiration should be in the order of shelter-belt trees irrigation, groundwater and cropland soil water. However, there were some uncertainties in calculating the contributions of groundwater and soil water to tree transpiration using the soil mass balance approach. Soil water in the cropland could diffuse into the shelter-belt trees stand. The lateral soil water movement term from cropland should be included as the water source in Eq. (7). This term might be quantified with the soil water potential gradient at the cropland-tree boundary and Darcy's law. Without consideration of this term due to the data unavailable, the soil water storage (S_1) would be underestimated, resulting in the overestimation of groundwater uptake (G_{up}) in Eq. (8) and

underestimation of soil water uptake (S_{up}) in Eq. (9). Therefore, the obtained contribution of groundwater in this study would be overestimated. Isotope tracing and model simulation approaches should be needed to accurately quantify the contributions of every water source for shelter-belt trees and substantially demonstrate the hydrological relations between tree and cropland, which is considered as the further scopes of this study.

The results about the groundwater uptake and cropland irrigation for Gansu Poplar transpiration in this study have important implications for the management of shelter-belt trees. The reduction of irrigation amount and frequency caused by the surface water shortage in the region will increase the dependence on groundwater resource. However, the over exploration of groundwater resource and the decline of water table depth will threaten the survival of the shelter-belt trees. As observed by Amlin and Rood (2003), *Populus balsamifera* displayed extensive leaf senescence and abscission because of the water table decline. Similar physiological and morphological responses to groundwater depletion were also reported for *Populus deltoids* (Cooper *et al*., 2003). Therefore, the proper and economical irrigation (such as drip irrigation or reasonable irrigation scheme with more irrigation events but less irrigation amount) instead of the conventional flood irrigation should be recommended for shelter-belt trees and cropland in the Heihe River Basin.

CONCLUSION

In this study, sap flow measurements were conducted on eight Gansu Poplar trees

with different diameter at breast height and distance from cropland during the growing seasons of 2012 and 2013. The sap flow variations and water use sources of shelter-belt trees were investigated. The following conclusions could be summarized. First, the mean sap flow density varied between 30.62±11.44 to 101.88±28.98 kg m^{-2} h^{-1}, and it increased linearly with the tree diameter at breast height. Second, the variations of sap flow density were mainly controlled by meteorological factors in addition to water table depth. Soil water had apparent influence on sap flow only after the shelter-belt trees irrigation. Third, the average stand transpiration during growing season was 4.9 mm d^{-1} in 2012 and 4.8 mm d^{-1} in 2013, respectively. The transpiration rate represented logarithmic relationship with reference crop evapotranspiration. Finally, the irrigation and precipitation was the main water use sources of shelter-belt trees, whereas groundwater and crop soil water provided importantly complementary water supply. The cropland irrigation could influence the tree transpiration within a threshold distance of about 8 m. Isotope tracing and model simulation approaches should be considered as the further study scopes to substantially quantify the contributions of different water use sources.

ACKNOWLEDGEMENT

This research was financially supported by the National Natural Science Foundation of China (91025018 and 91425301), and the 12th five year science and technology development program (2012BAC08B01). We would like to thank the Linze Inland River Basin Research Station Experimental for field experiment support. We thank the anonymous reviewers for their constructive comments which improved the overall quality of the manuscript.

REFERENCE

Allen RG, Pereira LS, Raes D, Smith M. 1998. Crop evapotranspiration (guidelines for computing crop water requirements). FAO Irrigation and drainage paper 56, Rome, Italy.

Amlin NM, Rood SB. 2003. Drought stress and recovery of riparian cottonwoods due to water table alteration along Willow Creek, Alberta. *Trees* **17**: 351-358.

Brooksbank K, Veneklaas EJ, White DA, Carter JL. 2011. Water availability determines hydrological impact of tree belts in dryland cropping systems. *Agricultural Water Management* **100**: 76-83.

Chang XX, Zhao WZ, Zhang ZH, Su YZ. 2006. Sap flow and tree conductance of shelter-belt in arid region of China. *Agricultural and Forest Meteorology* **138**: 132-141.

Chen DY, Wang YK, Liu SY, Wei XG. 2014. Response of relative sap flow to meteorological factors under different soil moisture conditions in rainfed jujube

(*Ziziphus jujube* Mill.) plantations in semiarid Northwest China. *Agricultural Water Management* **136**: 23-33.

Chen YN, Zhou HH, Chen YP. 2013. Adaptation strategies of desert riparian forest vegetation in response to drought stress. *Ecohydrology* **6**: 956-973.

Chirino E, Bellot J, Sánchez JR. 2011. Daily sap flow rate as an indicator of drought avoidance mechanisms in five Mediterranean perennial species in semi-arid southeastern Spain. *Trees* **25**: 593-606.

Cleverly JR, Smith SD, Sala A, Devitt DA. 1997. Invasive capacity of *Tamarix ramosissima* in a Mojave Desert floodplain: the role of drought. *Oecologia* **111**: 12-18.

Chu CR, Hsieh CI, Wu SY, Phillips NG. 2009. Transient response of sap flow to wind speed. *Journal of Experimental Botany* **60**: 249-255.

Cooper DJ, D'Amico DR, Scott ML. 2003. Physiological and morphological response patterns of *Populus deltoides* to alluvial groundwater pumping. *Environmental Management* **31**: 215-226.

Cramer VA, Thorburn PJ, Fraser GW. 1999. Transpiration and groundwater uptake from farm forest plots of *Casuarina glauca* and *Eucalyptus camaldulensis* in saline areas of southeast Queensland, Australia. *Agricultural Water Management* **39**: 187-204.

Dierick D, Hölscher D. 2009. Species-specific tree water use characteristics in reforestation stands in the Philippines. *Agricultural and Forest Meteorology* **149**: 1317-1326.

Du S, Wang YL, Kume T, Zhang J, Otsuki K, Yamanaka N, Liu GB. 2011. Sapflow characteristics and climatic responses in three forest species in the semiarid Loess Plateau region of China. *Agricultural and Forest Meteorology* **151**: 1-10.

Dzikiti S, Schachtschneider K, Naiken V, Gush M, Moses G, Le Maitre DC. 2013. Water relations and the effects of clearing invasive *Prosopis* trees on groundwater in an arid environment in the Northern Cape, South Africa. *Journal of Arid Environments* **90:** 103-113.

Eberbach PL, Burrows GE. 2006. The transpiration response by four topographically distributed *Eucalyptus* species, to rainfall occurring during drought in south eastern Australia. *Physiologia Plantarum* **127**: 483-493.

Gazal RM, Scott RL, Goodrich DC, Williams DG. 2006. Controls on transpiration in a semiarid riparian cottonwood forest. *Agricultural and Forest Meteorology* **137**: 56-67.

Glenn EP, Nagler PL, Morino K, Hultine KR. 2013. Phreatophytes under stress: transpiration and stomatal conductance of saltcedar (*Tamarix* spp.) in a high-salinity environment. *Plant and Soil* **371**: 655-672.

Gou S, Miller G. 2014. A groundwater-soil-plant-atmosphere continuum approach for modelling water stress, uptake, and hydraulic redistribution in phreatophytic vegetation. *Ecohydrology* **7**: 1029-1041.

Granier A. 1985. A new method of sap flow measurement in tree stems. *Annales des Sciences Forestières* **42**: 49-66.

Granier A. 1987. Evaluation of transpiration in a Douglas-fir stand by means of sap flow measurements. *Tree Physiology* **3**: 309-320.

Guan DX, Zhang XJ, Yuan FH, Chen NN, Wang AZ, Wu JB, Jin CJ. 2012. The relationship between sap flow of intercropped young poplar trees (*Populus*×*euramericana* cv. *N3016*) and environmental factors in a semiarid region of northeastern China. *Hydrological Processes* **26**: 2925-2937.

Liu B, Zhao WZ, Chang XX, Li SB, Zhang ZH, Du MW. 2009. Water requirements and stability of oasis ecosystem in arid region, China. *Environmental Earth Sciences* **59**: 1235-1244.

Liu B, Zhao WZ, Jin BW. 2011. The response of sap flow in desert shrubs to environmental variables in an arid region of China. *Ecohydrology* **4**: 448-457.

Luo F, Qi SZ, Xiao HL. 2005. Landscape change and sandy desertification in arid areas: a case study in the Zhangye Region of Gansu Province, China. *Environmental Geology* **49**: 90-97.

Ma JX, Huang X, Li WH, Zhu CG. 2013. Sap flow and trunk maximum daily shrinkage (MDS) measurements for diagnosing water status of *Populus euphratica* in an inland river basin of Northwest China. *Ecohydrology* **6**: 994-1000.

Motzer T, Munz N, Küppers M, Schmitt D, Anhuf D. 2005. Stomatal conductance, transpiration and sap flow of tropical montane rain forest trees in the southern Ecuadorian Andes. *Tree Physiology* **25**: 1283-1293.

Naithani KJ, Ewers BE, Pendall E. 2012. Sap flux-scaled transpiration and

stomatal conductance response to soil and atmospheric drought in a semi-arid sagebrush ecosystem. *Journal of Hydrology* **464-465**: 176-185.

O'Grady AP, Cook PG, Eamus D, Duguid A, Wischusen JD, Fass T, Worldege D 2009. Convergence of tree water use within an arid-zone woodland. *Oecologia* **160**: 643-655.

Pataki DE, Oren R, Smith WK. 2000. Sap flux of co-occurring species in a western subalpine forest during seasonal soil drought. *Ecology* **81**: 2557-2566.

Pinto CA, Nadezhdina N, David JS, Kurz-Besson C, Caldeira MC, Henriques MO, Monteiro FG, Pereira JS, David TS. 2013. Transpiration in *Quercus suber* trees under shallow water table conditions: the role of soil and groundwater. *Hydrological Processes* DOI: 10.1002/hyp.10097.

Plaut JA, Wadsworth WD, Pangle R, Yepez EA, McDowell NG, Pockman WT. 2013. Reduced transpiration response to precipitation pulses precedes mortality in a piñon-juniper woodland subject to prolonged drought. *New Phytologist* **200**: 375-387.

Prieto I, Kikvidze Z, Pugnaire FI. 2010. Hydraulic lift: soil processes and transpiration in the Mediterranean leguminous shrub *Retama sphaerocarpa* (L.) Boiss. *Plant and Soil* **329**: 447-456.

Raz-Yaseef N, Yakir D, Schiller G, Cohen S. 2012. Dynamics of evapotranspiration partitioning in a semi-arid forest as affected by temporal rainfall patterns. *Agricultural and Forest Meteorology* **157:** 77-85.

Rousseaux MC, Figuerola PI, Correa-Tedesco G, Searles PS. 2009. Seasonal

variations in sap flow and soil evaporation in an olive (*Olea europaea* L.) grove under two irrigation regimes in an arid region of Argentina. *Agricultural Water Management* **96**: 1037-1044.

Scanlon BR, Levitt DG, Reedy RC, Keese KE, Sully MJ. 2005. Ecological controls on water-cycle response to climate variability in deserts. *Proceedings of the National Academy of Sciences of the United States of America* **102**: 6033-6038.

Scott RL, James Shuttleworth W, Goodrich DC, Maddock III T. 2000. The water use of two dominant vegetation communities in a semiarid riparian ecosystem. *Agricultural and Forest Meteorology* **105**: 241-256.

Sellami MH, Sifaoui MS. 2003. Estimating transpiration in an intercropping system: measuring sap flow inside the oasis. *Agricultural Water Management* **59**: 191-204.

Shen Q, Gao GY, Fu BJ, Lü YH. 2014. Soil water content variations and hydrological relations of the cropland-treebelt-desert land use pattern in an oasis-desert ecotone of the Heihe River Basin, China. *Catena* **123**: 52-61.

Snyder KA, Williams DG. 2000. Water sources used by riparian trees varies among stream types on the San Pedro River, Arizona. *Agricultural and Forest Meteorology* **105**: 227-240.

Su YZ, Wang XF, Yang R, Lee J. 2010. Effects of sandy desertified land rehabilitation on soil carbon sequestration and aggregation in an arid region in China. *Journal of Environmental Management* **91**: 2109-2116.

Tognetti R, d'Andria R, Morelli G, Calandrelli D, Fragnito F. 2004. Irrigation effects on daily and seasonal variations of trunk sap flow and leaf water relations in olive trees. *Plant and Soil* **263**: 249-264.

Vincke C, Thiry Y. 2008. Water table is a relevant source for water uptake by a Scots pine (*Pinus sylvestris* L.) stand: Evidences from continuous evapotranspiration and water table monitoring. *Agricultural and Forest Meteorology* **148**: 1419-1432.

Williams DG, Cable W, Hultine K, Hoedjes JCB, Yepez EA, Simonneaux V, Er-Raki S, Boulet G, de Bruin HAR, Chehbouni A, Hartogensis OK, Timouk F 2004. Evapotranspiration components determined by stable isotope, sap flow and eddy covariance techniques. *Agricultural and Forest Meteorology* **125**: 241-258.

Woodall GS, Ward BH. 2002. Soil water relations, crop production and root pruning of a belt of trees. *Agricultural Water Management* **53**: 153-169.

Xu X, Tong L, Li F, Kang S, Qu Y. 2010. Sap flow of irrigated *Populus alba* var. *pyramidalis* and its relationship with environmental factors and leaf area index in an arid region of Northwest China. *Journal of Forest Research* **16:** 144-152.

Zhang YQ. Kang SZ, Ward EJ, Ding RS, Zhang X, Zheng R. 2011. Evapotranspiration components determined by sap flow and microlysimetry techniques of a vineyard in northwest China: Dynamics and influential factors. *Agricultural Water Management* **98**: 1207-1214.

Zhao WZ, Liu B. 2010. The response of sap flow in shrubs to rainfall pulses in the desert region of China. *Agricultural and Forest Meteorology* **150**: 1297-1306.

Table I. Overview of previous studies regarding forest and shrub transpiration in arid and semiarid area.

Location	Precipitation/ mm	Groundwater/ m	Plant types	Methods	References
Alicante, Southeastern Spain (38°28′N, 0°37′W)	275	-	Shrub (*Quercus coccifera, Pistacia lentiscus, Erica multiflora*), Tree (*Pinus halepensis*)	HBM	Chirino *et al*., 2011
Almería, Southeastern Spain (37°08′N, 2°22′W)	250	-	Shrub (*Retama sphaerocarpa*)	HBM	Prieto *et al*., 2010
Judean Mountain ridge, Southern Israel (31°21′N, 35°02′E)	285±88	>300	Tree (*Pinus halepensis*)	HPV, TDM	Raz-Yaseef *et al*., 2012
Marrakech, Morocco (31°36′N, 07°58′W)	253	-	Olive orchard (*Olea europaea*)	HPV, IBM, ECM	Williams *et al*., 2004
Northern Cape, South Africa (29.36°S, 21.19°E)	75-200	7-12	Tree (*Prosopis* spp.)	HPV, ECM	Dzikiti *et al*., 2013
Northern Territory, Australia (21°54′S, 133°51′E and 22°20′S, 133°19′E)	300	7, 40	Tree (*Corymbia opaca, Eucalyptus victrix, Acacia aneura, Eucalyptus camaldulensis*)	HPV	O'Grady *et al*., 2009
La Rioja, Argentina (28°33′S, 66°49′W)	-	-	Olive orchard (*Olea europaea*)	HBM	Rousseaux *et al*., 2009
Mojave Desert, Southern Nevada (36°40′N, 114°20′E)	100	> 0.1	Riparian forests (*Tamarix ramosissima, Pluchea sericea, Prosopis pubescens, Salix exigua*)	HBM	Cleverly *et al*., 1997

Arizona, U.S. (31°33′N, 110°07′W)	330	1.8-4.2	Riparian forests (*Salix gooddingii*, *Populus fremontii*), Shrub (*Prosopis velutina*)	IBM	Snyder and Williams, 2000
Wyoming, U.S. (41°21′23″N, 107°23′33″W)	259-341	-	Shrub (*Artemisia tridentata* var. *vaseyana*)	HBM	Naithani *et al.*, 2012
Colorado River, U.S. (33°16′N, 114°41′W)	< 100	2.4-3.6	Riparian subshrub (*Tamarix* spp.)	HBM, TDM	Glenn *et al*., 2013
New Mexico, U.S. (34°23′11″N, 106°31′46″W)	358	-	Forest (*Pinus Edulis*, *Juniperus monosperma*)	TDM	Plaut *et al*., 2013
Liaoning, Northeast China (41°46′55″N, 119°17′24″E)	450	2	Agroforestry (*Populu seuramericana* cv. *N3016*)	TDM	Guan *et al*., 2011
Loess Plateau, Shaanxi, China (36°25.40′N, 109°31.53′E)	498	-	Forest (*Robinia pseudoacacia*, *Quercus liaotungensis*, *Armeniaca sibirica*)	TDM	Du *et al*., 2011
Shiyanghe River, Northwest China (37°52′20″N, 102°50′50″E)	164	25-30	Farmland shelter-belt (*Populus alba* var. *pyramidalis*)	HPV	Xu *et al*., 2010
Middle of Heihe River basin, Northwest China (39°21N, 100°07′E)	117	>2.8	Farmland shelter-belt (*Populus gansuensis*)	HPV	Chang *et al*., 2006
			Desert shrub (*Nitraria sphaerocarpa*, *Elaeagnus angustifolia*)	HBM	Liu *et al*., 2011

Note: HBM, HPV, TDM, IBM and ECM stood for heat balance method, heat pulse velocity method, thermal dissipation method, isotope-based method, eddy covariance measurement method, respectively.

Table II. Parameters of the eight sample trees used for sap flow measurement in the shelter-belt trees stand.

No.	Diameter at breast height (cm)	Sapwood area (cm^2)	Canopy projected area (m^2)
1	36	620.908	20.2
2	30	465.430	30.4
3	32	517.256	7.2
4	38	672.734	15.0
5	24	309.952	14.4
6	21	232.213	4.6
7	27	387.691	9.9
8	22	258.126	4.8

Table III. Soil physical properties of different soil layers in the shelter-belt trees stand.

Soil layer (cm)	Sand (%)	Silt (%)	Clay (%)	Bulk density (g/cm^3)	Wilting coefficient (%)	Field capacity (%)
0-20	86.54	12.13	1.34	1.26	5.45	9.15
20-160	91.90	7.38	0.72	1.59	4.55	7.89
160-220	87.15	11.61	1.24	1.65	6.10	9.46
220-280	70.76	26.89	2.35	1.70	11.09	20.38

Table IV. Spearman's rank correlation coefficients between sap flow density and different environment factors during two growing seasons of Gansu Poplar in 2012 and 2013.

	SF_d	T_a	RH	P	R_g	VPD	WTD	REW
SF_d		**0.35****	**-0.32****	**-0.32****	**0.67****	**0.44****	**-0.43****	**0.58****
T_a	0.47**		**-0.26****	**-0.31****	**0.58****	**0.81****	**-0.10**	**0.22***
RH	-0.02	0.14		**0.68****	**-0.27****	**-0.74****	**-0.17**	**-0.22***
P	-0.10	-0.15	0.50**		**-0.39****	**-0.59****	**-0.18**	**-0.03**
R_g	0.67**	0.37**	-0.25**	-0.23*		**0.55****	**-0.14**	**0.39****
VPD	0.40**	0.68**	-0.59**	-0.42**	0.45**		**0.04**	**0.31****
WTD	-0.50**	-0.45**	-0.18*	-0.08	-0.20*	-0.19*		**-0.47****
REW	0.47**	0.49**	0.14	0.04	0.10	0.25**	-0.92**	

Notes: (a) SF_d: sap flow density (kg m^{-2} h^{-1}), T_a: air temperature (^oC), RH: relative humidity, P: precipitation (mm), R_g: solar radiation (MJ m^{-2}), VPD: vapor pressure deficit (KPa), WTD: water table depth (m), REW: relative extractable water.

(b) '*' indicates correlation is significant at the 0.05 level (2-tailed), '**' indicates correlation is significant at the 0.01 level (2-tailed).

(c) Coefficients in lower triangular belong to 2012 growing season, and the ones in bold in upper triangular belong to 2013 growing season.

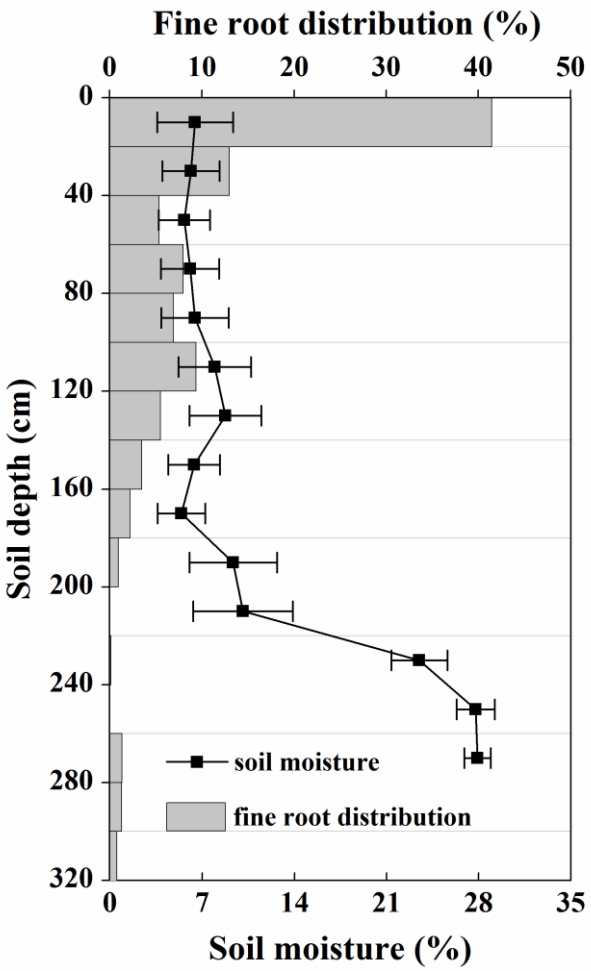

Figure 1. The vertical profile distribution of mean soil moisture (0-280 cm) during growing seasons in 2012 and 2013, and fine root biomass of Gansu Poplar (0-320 cm) measured on 23th August of 2013.

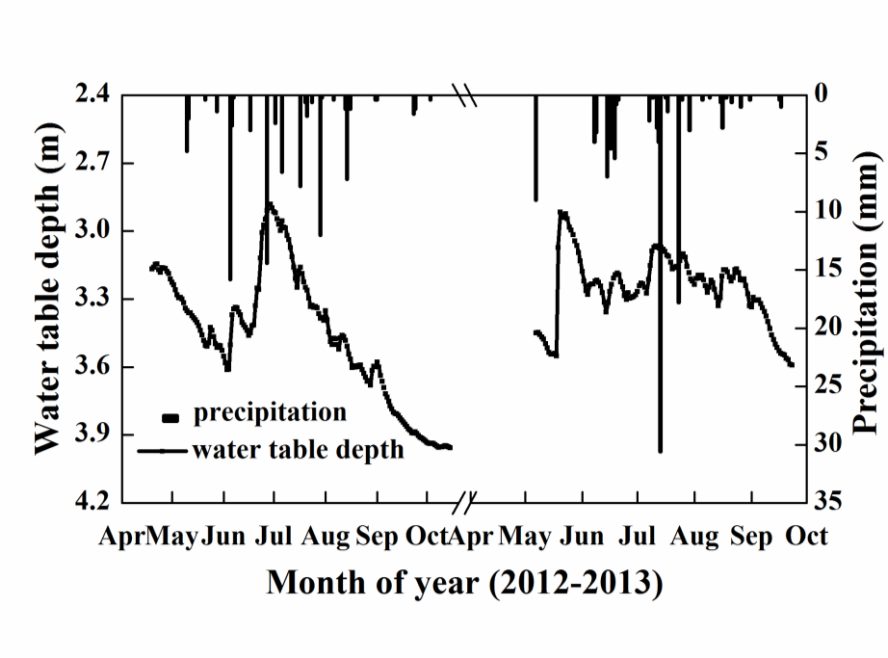

Figure 2. The precipitation distribution and water table depth during two growing seasons of Gansu Poplar in 2012 and 2013.

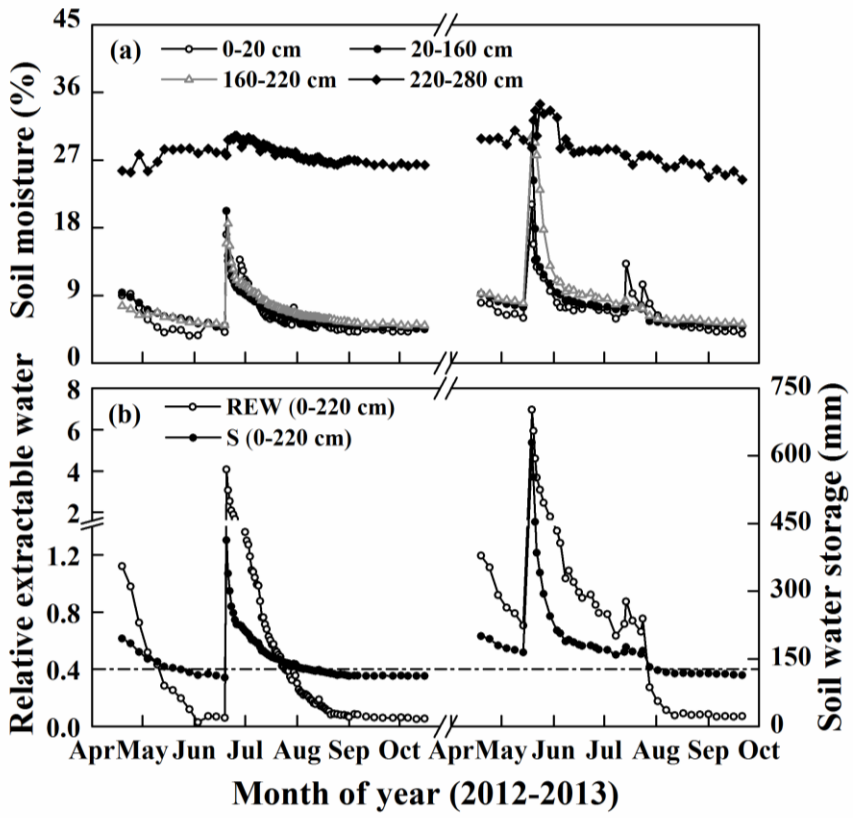

Figure 3. The temporal variations of (a) soil moisture at four soil layers (0-20, 20-160, 160-220, 220-280 cm), and (b) relative extractable water (REW) and soil water storage (*S*) at the depth of 0-220 cm. The horizontal line (REW=0.4) stood for the threshold of soil moisture deficit.

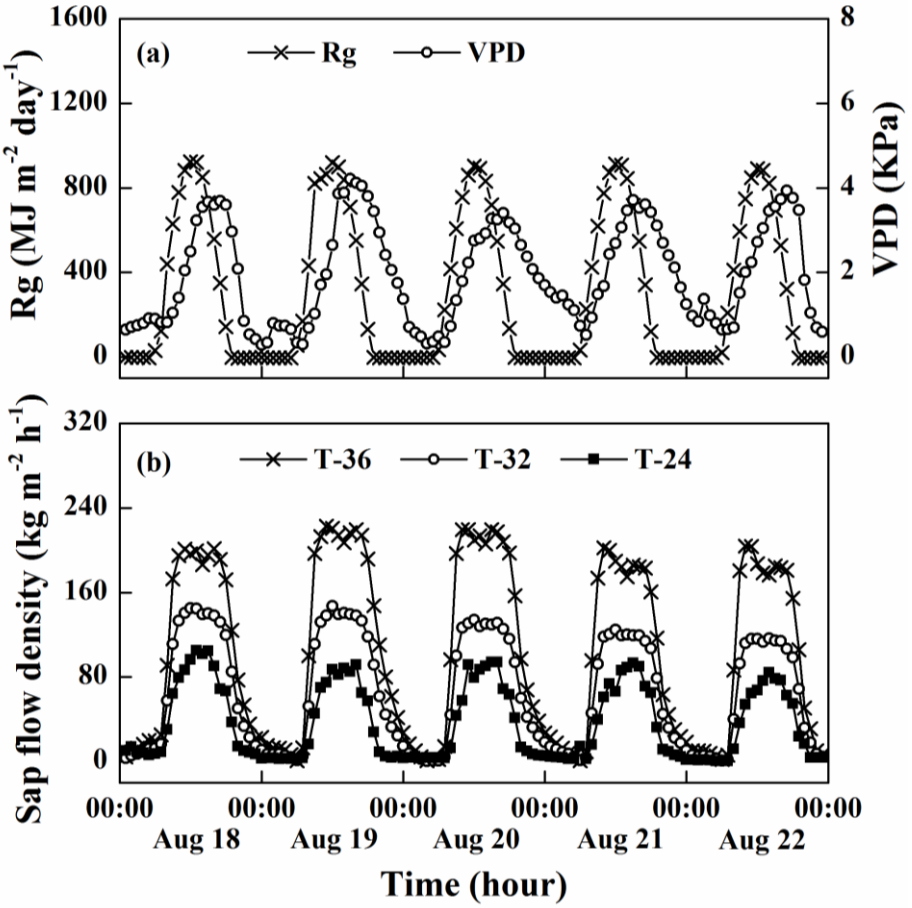

Figure 4. Diurnal time courses of (a) solar radiation (R_g) and vapor pressure deficit (VPD), and (b) sap flow density (SF_d) of trees with different diameter at breast height (24, 32 and 36 cm) and different distance from the cropland (6.3, 8.1 and 13.5 m) on five successive days in 2012.

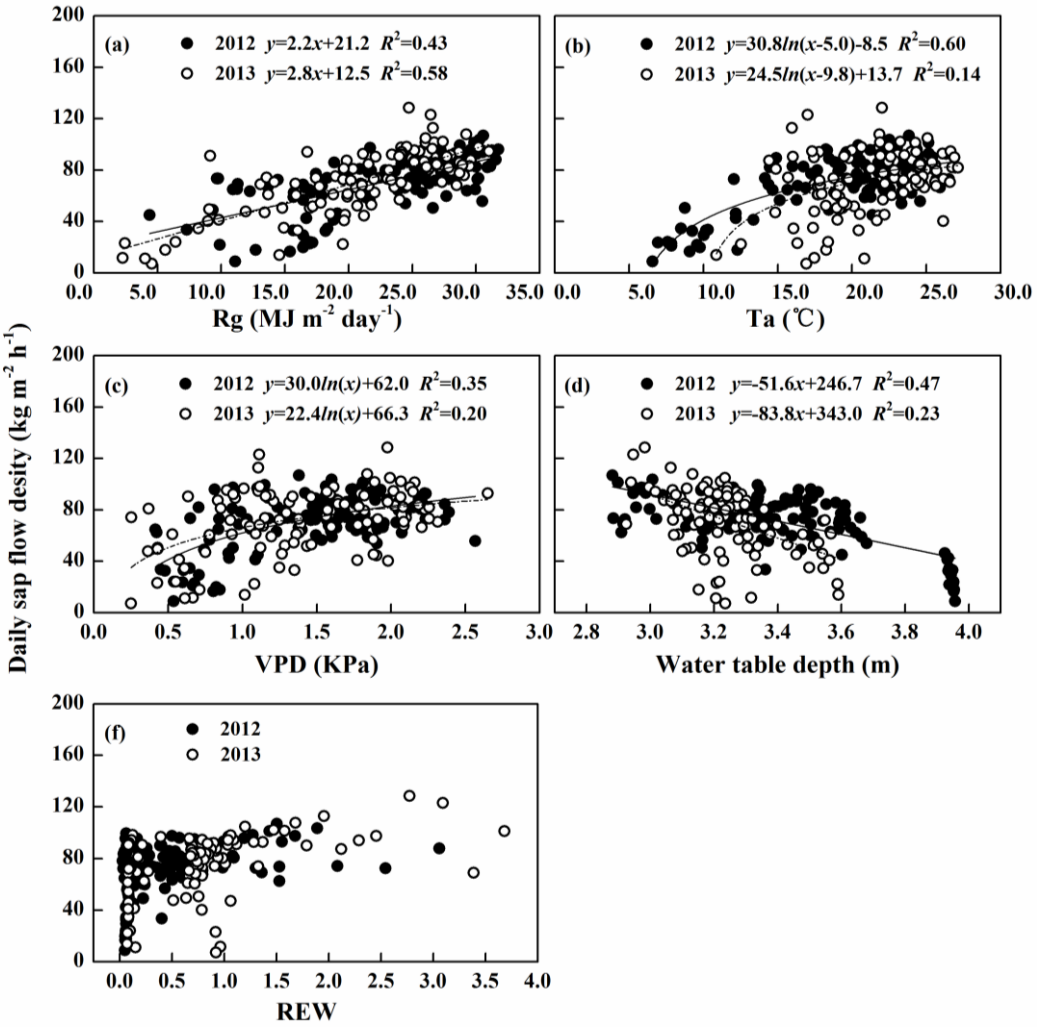

Figure 5. The relationship between daily sap flow density and (a) solar radiation (R_g), (b) air temperature (T_a), (c) vapor pressure deficit (VPD) ,(d) water table depth and (e) relative extractable water (REW) during two growing seasons of Gansu Poplar in 2012 and 2013.

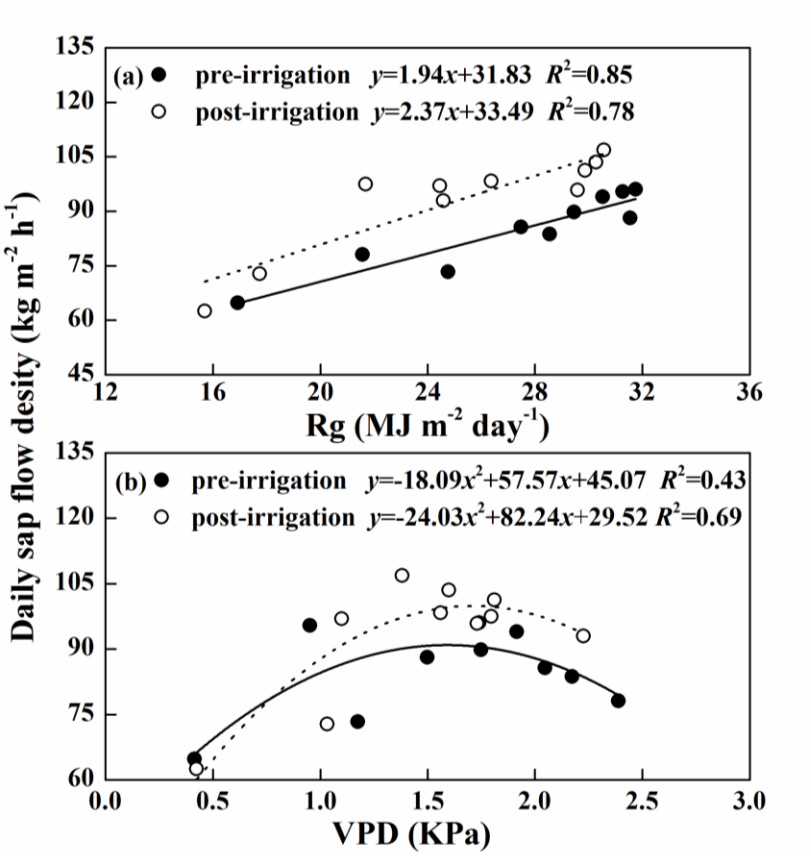

Figure 6. The relationship between daily sap flow density and (a) solar radiation (R_g), and (b) vapor pressure deficit (VPD) during the shelter-belt trees pre-irrigation (10th-19th, June) and post-irrigation (21th-30th, June) periods in 2012.

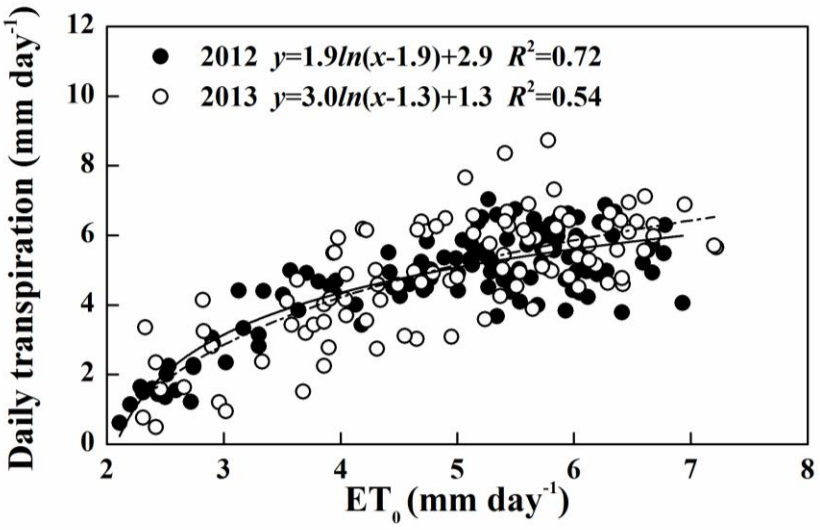

Figure 7. The relationship between daily transpiration (mm day^{-1}) and reference evapotranspiration (ET_0, mm day^{-1}) during two growing seasons of Gansu Poplar in 2012 and 2013.

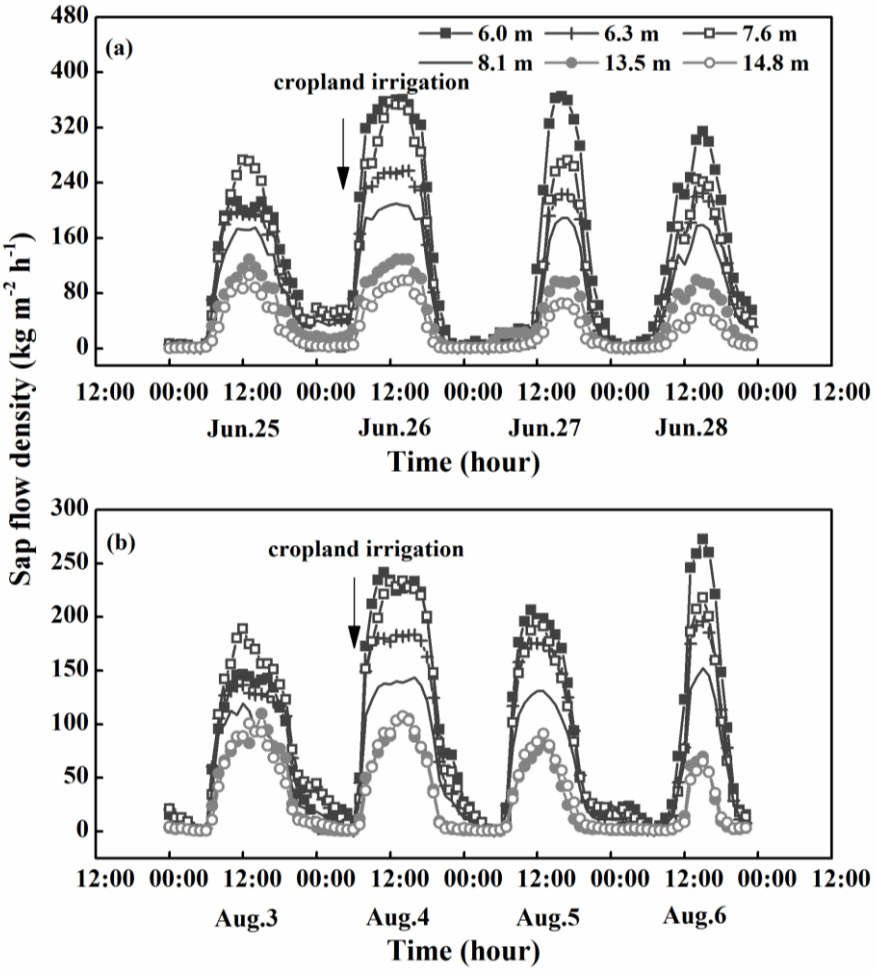

Figure 8. The response of shelter-belt sap flow variations to cropland irrigation events for successive three days in 2012. The sample trees had distances of 6.0, 6.3, 7.6, 8.1, 13.5 and 14.8 m from the cropland.